BIOLOGY OF REPRODUCTION **82,** 86–95 (2010)
Published online before print 19 August 2009.
DOI 10.1095/biolreprod.109.078543

Effects of Neonatal Exposure to Bisphenol A on Steroid Regulation of Vascular Endothelial Growth Factor Expression and Endothelial Cell Proliferation in the Adult Rat Uterus[1]

Verónica L. Bosquiazzo, Jorgelina Varayoud, Mónica Muñoz-de-Toro, Enrique H. Luque, and Jorge G. Ramos[2]

Laboratorio de Endocrinología y Tumores Hormonodependientes, School of Biochemistry and Biological Sciences, Universidad Nacional del Litoral, Santa Fe, Argentina

ABSTRACT

Hormonally controlled vascular changes play a key role in endometrial development and in the differentiation process necessary for implantation. Vascular endothelial growth factor (VEGF) has emerged as one of the central regulators of the uterine vasculature. Hormonal perturbations during neonatal development may alter sex steroid-dependent regulation of VEGF and may ultimately affect fertility later in life. The aim of this study was to determine whether neonatal exposure to the environmental estrogenic chemical bisphenol A (BPA) affects the adult rat uterine response to hormonal stimuli. Newborn female rats were given s.c. injections of vehicle, BPA (0.05 mg/kg per day or 20 mg/kg per day) or diethylstilbestrol (0.2 μg/kg per day) on Postnatal Days 1, 3, 5, and 7. To evaluate the long-term effects, rats were ovariectomized at Postnatal Day 80 and submitted to hormonal replacement. Rats neonatally exposed to xenoestrogens showed a decreased induction of uterine endothelial proliferation and a decreased *Vegf* mRNA expression in response to ovarian steroid treatment. Also, although the estrogen receptor alpha (ESR1) expression was lower in subepithelial cells than in controls, a higher expression of silencing mediator of retinoic acid and thyroid hormone receptor (NCOR1, also known as SMRT) corepressor was evidenced in the same compartment. The results indicate that disturbed *Vegf* expression in BPA rats could be the result of changes in endocrine pathways, such as an altered induction of ESR1 and/or NCOR1 expression. Because of the importance of VEGF in the implantation process, our data suggest that neonatal BPA exposure might have negative consequences on female fertility.

bisphenol A, endothelial cell proliferation, environment, female reproductive tract, steroid hormone receptors, toxicology, uterus, vascular endothelial growth factor

INTRODUCTION

In the uterus, the formation of new maternal blood vessels in the stromal compartment at the time of embryonic implantation is critical for the establishment and maintenance of pregnancy. Uterine angiogenesis is known to be influenced by the steroid hormones 17β-estradiol (E_2) and progesterone (P4) through activation of their respective nuclear receptors [1, 2]. The sex steroid-receptor complex exerts some biological effects indirectly via a variety of growth factors [3]. Among them, vascular endothelial growth factor (VEGF) is likely the main factor responsible for the vascular permeability and angiogenesis during the peri-implantation period. Female mice treated with VEGF antiserum on the fourth day after mating showed that pregnancy was blocked [4, 5], which is evidence of the key role of VEGF in the preparation of the endometrium for embryo implantation. In addition, immunoneutralization of VEGF inhibits pregnancy establishment in the rhesus monkey [6].

VEGF is present in different uterine cellular compartments, and its differential expression is associated with ovarian steroid levels. Studies in three different rodent species have shown that the luminal epithelium is the site of increased VEGF expression in the uterus in response to E_2 [7–9]. In addition, these studies showed little or no VEGF expression in stromal tissue until after P4 administration. Different results have shown that P4- and E_2-induced uterine *Vegf* expression did not involve progesterone receptor (PGR) or estrogen receptor (ESR1) interactions with their classic consensus hormone response element [10, 11]. Thus, in the rat uterus, E_2 induces the recruitment of ESR1 to the proximal GC-rich region of the *Vegf* promoter, probably via interaction with SP proteins [10]. In endometrial adenocarcinoma cells (Ishikawa cells), PGR-mediated transcriptional regulation of the *Vegf* is complex and cannot be localized to confined P4 response elements sequences, suggesting that other alternative transcription factors play an important role in the regulation of *Vegf* by P4 [11]. Therefore, downstream *Vegf* regulation by ovarian hormones depends on the expression profiles and recruitment of different transcription factors to the *Vegf* promoter region.

The hormonal perturbation during fetal or neonatal development may predispose individuals to disease and/or dysfunction later in life. A large number of studies reported significant effects of exposure to xenoestrogenic substances, such as bisphenol A (BPA), on estrogen-sensitive organs [12]. Bisphenol A is used to manufacture polycarbonate plastics and epoxy resins used in the manufacture of dental fillings, baby bottles, and food packaging. Leaching of BPA increases with repeated use or exposing the polycarbonate products to high temperatures [13]. Recent studies showed that developmental exposure to BPA affects the histology and steroid hormone

[1]Supported by grants from the Universidad Nacional del Litoral (CAI+D program) and the Argentine National Agency for the Promotion of Science and Technology. V.L.B. is a fellow, and J.V., E.H.L., and J.G.R. are Career Investigators of the Argentine National Council for Science and Technology.
[2]Correspondence: Jorge G. Ramos, Laboratorio de Endocrinología y Tumores Hormonodependientes, School of Biochemistry and Biological Sciences, Casilla de Correo 242, (3000) Santa Fe, Argentina.
FAX: 54 342 4575207; e-mail: gramos@fbcb.unl.edu.ar

Received: 29 April 2009.
First decision: 24 May 2009.
Accepted: 7 August 2009.

eISSN: 1529-7268 http://www.biolreprod.org
ISSN: 0006-3363

responsiveness of uterine stroma in the adult [14–16]. These effects may be associated with a deregulation of steroid receptor expression or an alteration in the transcription machinery's assembly that subsequently would alter the expression of estrogen-sensitive genes [14, 16]. Consistent with this, Long et al. [17] showed that BPA rapidly stimulated expression of *Vegf* in the classic estrogen-responsive tissues of the rat, such as the uterus, the vagina, and the pituitary. In addition, an in vitro study showed that BPA upregulated *Vegf* expression in MELN cells by an ESR-dependent mechanism [18].

In the present work, we used an experimental protocol to investigate the long-term effects of neonatal BPA exposure on steroid hormone regulation of uterine vascular events. We used an ovariectomized (OVX) adult rat model treated with P4 and E_2 that closely mirrors the endocrine and molecular changes found in the preimplantation period [19]. Specifically, we determined whether neonatal BPA impairs steroid regulation of *Vegf* expression and endothelial proliferation as central events of endometrial vascularization. Given that these events are regulated by steroid hormones acting via their nuclear receptors, we also examined the expression of ESR1, PGR, and coregulator proteins to evaluate whether the endocrine pathway is affected.

MATERIALS AND METHODS

Animals

All animal procedures were performed in accordance with the principles and guidance outlined in the Guide for the Care and Use of Laboratory Animals issued by the U.S. National Academy of Sciences. Rats of an inbred Wistar-derived strain bred at the Department of Human Physiology (Universidad Nacional del Litoral, Santa Fe, Argentina) were maintained under a controlled environment (22°C ± 2°C; lights on from 600 to 2000 h) and had free access to pellet laboratory chow (Nutrición Animal, Santa Fe, Argentina) and tap water. The concentration of phytoestrogens in the diet was not evaluated; however, because food intake was very similar in the control and experimental rats (Bosquiazzo et al., unpublished observations), we assumed that all animals were exposed to the same levels of food-borne phytoestrogens. To minimize additional exposures to endocrine-disrupting chemicals, rats were housed in stainless steel cages with wood bedding, and tap water was supplied in glass bottles with rubber stoppers surrounded by a steel ring.

Experimental Design

Pregnant rats were housed singly. Upon delivery, pups were sexed according to anogenital distance and were cross fostered, distributing the female pups of each litter among different mothers (adjusting the number of pups to five females and five males whenever possible). These actions allowed us to minimize the use of siblings to avoid potential litter effects. Female pups from each foster mother were assigned to one of the following neonatal treatments (eight pups per group; Fig. 1): 1) controls given corn oil vehicle alone, 2) diethylstilbestrol (DES; Sigma, St. Louis, MO) at 0.2 μg/kg per day, 3) BPA (99% purity; Sigma-Aldrich, Milwaukee, WI) at 20 mg/kg per day (BPA20), or 4) BPA at 0.05 mg/kg per day (BPA.05). Treatments were given on Postnatal Days (PNDs) 1, 3, 5, and 7 (day of birth = 0) by s.c. injections in the nape of the neck. Male pups were used in another experiment. No signs of acute or chronic toxicity were observed, and no significant differences in weight gain between xenoestrogen-exposed and control pups were recorded during the experiment. Female pups were weaned at 21 days of age and housed four per cage until 80 days of age (Fig. 1).

Ovariectomy and Hormonal Treatment

A pilot experiment using OVX adult rats was performed to optimize hormone replacement treatment. The schedule of hormone administration was adapted from a previous study which showed that P4 pretreatment followed by a physiological dose of E_2 increased the number of proliferating rat uterine stromal cells, such as happens in normally pregnant animals [19]. Ten days after OVX, rats were treated (s.c.) as follows: a daily dose of P4 (10 mg/kg; Sigma) on the first and second day, followed by a dose of P4 (10 mg/kg) plus E_2 (4 μg/kg; Sigma) on the third day (OVX-P4 + E_2 group; n = 5). Another set

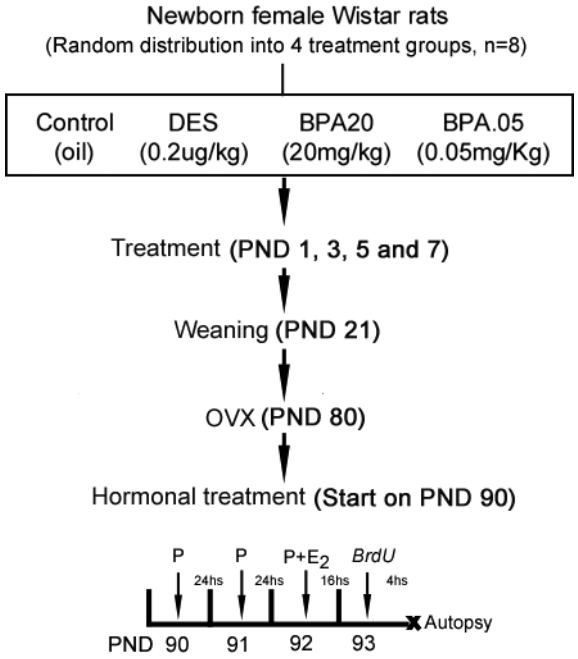

FIG. 1. Schematic representation of experimental design. P, progesterone; X, time of autopsy.

of rats received daily doses of vehicle (OVX group; n= 5). Sixteen hours after the last treatment dose, each rat was injected (i.p.) with the thymidine analog bromodeoxyuridine (BrdU; 60 mg/kg; Sigma). The set of rats neonatally exposed to corn oil, DES, and BPA (BPA.05 and BPA20), which had been housed until 80 days of age, were OVX and treated with the above-described steroid replacement treatment (n = 8 rats per group). Uterine tissues were harvested 4 h after the BrdU injection. One uterine horn from each rat was placed immediately in liquid nitrogen and stored at −80°C for RNA extraction. The other uterine horn was weighed and then fixed by immersion in 10% buffered formalin for 6 h at 4°C, embedded in paraffin, and used for immunohistochemical and immunofluorescence staining.

RNA Extraction and RT

Individual uterine horn samples were homogenized in TRIzol (Invitrogen, Carlsbad, CA), and RNA was prepared according to the manufacturer's protocol. The concentration of total RNA was assessed by A260, and the samples were stored at −80°C until needed. Equal quantities (4 μg) of total RNA were reverse transcribed into cDNA with AMV reverse transcriptase (12.5 units; Promega, Madison, WI) using 200 pmol of random primers (Promega). Twenty units of ribonuclease inhibitor (RNAout; Invitrogen Argentina, Buenos Aires, Argentina) and 100 nmol of a deoxynucleotide triphosphate (dNTP) mixture was added to each reaction tube in a final volume of 30 μl of 1× AMV-RT buffer. Reverse transcription was performed at 42°C for 90 min. The reactions were stopped by heating at 97°C for 5 min and cooling on ice, followed by dilution of the reverse-transcribed cDNA with RNAse-free water to a final volume of 60 μl. The samples were analyzed in triplicate, and a sample without reverse transcriptase was included to detect contamination by genomic DNA.

PCR Analysis

Vegf *mRNA expression*. To evaluate the *Vegf* mRNA expression, we performed real-time PCR reactions using protocols described previously [20]. Primer pairs used for amplification of *Vegf* and the ribosomal protein 19, *Rpl19* (housekeeping gene), cDNAs are shown in Table 1 [21, 22]. The cDNA levels were detected using real-time PCR with the DNA Engine Opticon System (Bio-Rad Laboratories Inc., Waltham, MA) and SYBR Green I dye (Cambrex Corp., East Rutherford, NJ). For cDNA amplification, 5 μl of cDNA was combined with a mixture containing 2.5 units of Taq-DNA polymerase (Invitrogen), 2 mM $MgCl_2$ (Invitrogen), 0.2 mM each of the four dNTPs (Promega), and 10 pmol of each primer (Invitrogen) in a final volume of 25 μl of 1× SYBR Green I PCR Taq buffer. After initial denaturation at 97°C for 1 min, the reaction mixture was subjected to successive cycles of denaturation at 97°C for 45 sec,

TABLE 1. Sequences of PCR primers.

Primer	Sequence	Product size
Vegf sense	5′-CTGCTCTCTTGGGTGCACTGG-3′	320 bp
Vegf antisense	5′-GGTTTGATCCGCATGATCTGCAT-3′	
Vegf isoform sense	5′-CATGCGGATCAAACCTCACC-3′	*Vegf_120*: 126 bp
Vegf isoform antisense	5′-CACCGCCTTGGCTTGTCACA-3′	*Vegf_164*: 258 bp *Vegf_188*: 330 bp
Rpl19 sense	5′-GAAATCGCCAATGCCAACTC-3′	290 bp
Rpl19 antisense	5′-ACCTTCAGGTACAGGCGTTG-3′	

annealing at 60°C (*Vegf*) and 55°C (*Rpl19*) for 1 min, and extension at 72°C for 1 min. Product purity was confirmed by dissociation curves, and random samples were subjected to agarose gel electrophoresis. All PCR products were cloned using a TA cloning kit (Invitrogen), and the specificity was confirmed by DNA sequencing (data not shown). Calculation of the relative expression levels of each target was conducted based on the cycle threshold (C_T) method [23]. The C_T for each sample was calculated using the Opticon Monitor Analysis Software (MJ Research) with an automatic fluorescence threshold (R_n) setting. Accordingly, fold expression over control values was calculated for each target by the equation $2^{-\Delta\Delta CT}$, where ΔC_T is determined by subtracting the corresponding *Rpl19* C_T value (internal control) from the specific C_T of each gene target, and $\Delta\Delta C_T$ is obtained by subtracting the ΔC_T of each experimental group from that of the control group (taken as reference value 100). No significant differences in C_T values were observed for *Rpl19* between the different experimental groups.

Analysis of Vegf mRNA splice variant expression. To coamplify the main *Vegf* mRNA splice variants (120, 164, and 188), we performed a PCR with specific primers located flanking the alternative splicing sites corresponding to exons 6 and 7 of the *Vegf* cDNA sequence [24]. For cDNA amplification, 5 μl of cDNA was combined with a mixture containing 2.5 units of Taq DNA polymerase, 1 mM $MgCl_2$, 0.2 mM each of the four dNTPs, and 20 pmol of each *Vegf*-specific primer (Invitrogen; Table 1) in a final volume of 25 μl of 1× PCR Taq buffer (Invitrogen). The PCRs were performed as described previously, using an annealing temperature of 61°C. Melting curves showed the absence of heteroduplex formation and unspecific amplification products [25]. The PCR products were resolved on 2% (w/v) agarose gels, cloned, and sequenced (data not shown). Agarose gel images were digitized using a Sony ExwaveHAM color video camera (Sony Electronics Inc., Park Ridge, NJ) and the Image Pro-Plus 4.1.0.1 image system analyzer (Media Cybernetics). The relative expression of each splice variant was evaluated by determining the integrated optical density (IOD) by densitometry.

Immunohistochemistry

Antibodies. The anti-VEGF antibody (clone C-1; 1:50 dilution) was purchased from Santa Cruz Biotechnology Inc. (Santa Cruz, CA). The anti-nestin antibody (clone rat 401; 1:200 dilution) was purchased from BD Pharmingen (San Jose, CA). The affinity-purified antibodies for ESR1 (clone 6F-11; 1:200 dilution) and BrdU (clone 85–2C8; 1:100 dilution) were purchased from Novocastra (Newcastle upon Tyne, U.K.). The anti-PGR antibody (A0098; 1:500 dilution) and von Willebrand factor (VWF; 1:200 dilution) were purchased from Dako Corp. (Carpinteria, CA). The affinity-purified rabbit polyclonal antibodies for steroid receptor coactivator 3 (NCOA3; 1:150 dilution) and for the silencing mediator of retinoic acid and thyroid hormone receptors (NCOR1; 1:50 dilution) were generated and tested in our laboratory [16]. Anti-rabbit and anti-mouse secondary antibodies (biotin conjugate; B8895/B8774; 1:200 dilution) were purchased from Sigma. For dual-immunofluorescence staining, the secondary antibodies were AlexaFluor 488 goat anti-rabbit (green; A-11034; 1:100 dilution; Invitrogen), Cy2-conjugated goat anti-mouse (green; 155-225-003; 1:100 dilution), and TRITC-conjugated anti-rabbit (red; 016-020-084; 1:200 dilution; Jackson ImmnoResearch, West Grove, PA).

Single immunohistochemistry. Uterine sections (5 μm in thickness) were deparaffinized and dehydrated in graded ethanols. Immunostaining for VEGF, nestin, VWF, ESR1, PGR, NCOR1 (SMRT), and NCOA3 (SRC-3) was performed as described previously [26]. In brief, after microwave pretreatment for antigen retrieval, endogenous peroxidase activity and nonspecific binding sites were blocked. The primary antibodies were incubated overnight at 4°C. After incubation with biotin-conjugated secondary antibodies for 30 min, the reactions were developed using a streptavidin-biotin peroxidase method and diaminobenzidine (Sigma) as a cromogen substrate. The samples were counterstained with Mayer hematoxylin (Biopur, Rosario, Argentina) and mounted with permanent mounting medium (PMyR, Buenos Aires, Argentina). Each immunohistochemical run included negative controls. For negative controls, the primary antibody was replaced with nonimmune serum (Sigma). For NCOA3 and NCOR1 immunostaining, the antigenic peptides were used to preadsorb NCOA3 and NCOR1 antibodies by incubating 1 μg of antibody with 10–20 μg of peptide for 24 h at 4°C. The antibody-antigen complexes were applied in immunohistochemical assays to positive control tissues.

Quantification of single immunohistochemistry by image analysis. Tissue sections were evaluated using a BH2 microscope (illumination: 12-V halogen lamp, 100 W, equipped with a stabilized light source; Olympus, Tokyo, Japan) with the Dplan 40× objective (numerical aperture, 0.65; Olympus). To measure the vascular areas and the IOD of PGR, ESR1, NCOR1, and NCOA3 immunostaining in the subepithelial stroma, image analysis was performed using the Image Pro-Plus 4.1.0.1 system (Media Cybernetics, Silver Spring, MD), as described previously [27–29]. In brief, the images were recorded with a Spot Insight version 3.5 color video camera (Diagnostic Instruments, Sterling Heights, MI). At least 10 fields were recorded in each section, and two sections per animal were evaluated. The correction of unequal illumination (shading correction) and the calibration of the measurement system were done with a reference slide. The images of immunostained slides were converted to a gray scale, and the subepithelial stromal compartment was delimited (a 300-μm-wide area adjacent to the epithelium from the basement membrane toward the outer layers). Using the Auto-Pro macro language, an automated standard sequence operation was created to measure the vascular areas and IOD.

The subepithelial vascular area was calculated by dividing the sum of the area occupied by individual vessels (measured using the immunostaining for VWF) by the total area occupied by the subepithelial stroma.

The nestin-expressing vascular area was obtained by dividing the area occupied by nestin-positive vessels by the positive VWF vascular area. This parameter indicates the relative area occupied by those blood vessels that are capable of proliferating in the presence of a stimulus [30, 31].

The IOD of PGR, ESR1, NCOR1, and NCOA3 was evaluated as a linear combination between the average gray optical density and the relative area occupied by positive cells on sections without hematoxylin counterstaining.

Because vascular areas and IOD are dimensionless parameters, the results were expressed as arbitrary units.

Double immunohistochemistry. A sequential double-immunoassay technique was employed to identify the proliferating (BrdU-positive) or steroid receptor-expressing endothelial cells [32]. BrdU incorporation to detect cells in the S phase of the cell cycle was done as described previously [33]. PGR and ESR1 detection was performed as described above. After the first immunoreaction, sections were microwave heated to wash out any remaining antibodies from the former assay. Sections were rinsed with PBS and preincubated with normal goat antiserum for 30 min [32]. Samples were then incubated overnight at 4°C with an anti-nestin antibody to detect the subpopulation of endothelial cells that are capable of proliferating [30, 31]. Immunohistochemistry (IHC) reactions were developed using a streptavidin-biotin peroxidase method. Visualization of nestin-positive cells was achieved by the nickel-intensified diaminobenzidine technique. Slides were counterstained with Nuclear Fast Red and mounted with permanent mounting medium. Proliferating or steroid receptor-expressing endothelial cells exhibited brown-stained nuclei (BrdU, ESR1, or PGR positive), whereas nestin-positive cells were identified by a black-stained cytoplasm.

Quantification of proliferating and steroid receptor-positive endothelial cells. Tissue sections were evaluated using the Olympus BH2 microscope with a Dplan 100× objective (numerical aperture = 1.25; Olympus). The percentage of proliferating or steroid receptor-expressing endothelial cells was examined on sections double immunostained for BrdU, PGR or ESR1, and nestin and was calculated by dividing the number of double-positive endothelial cells by the total number of nestin-positive endothelial cells. Two sections of each uterus were analyzed, and approximately 100 nestin-positive vessels per section were quantified.

Double immunofluorescence. Double labeling was conducted using combinations of the antibodies listed above. Uterine sections were deparaffi-

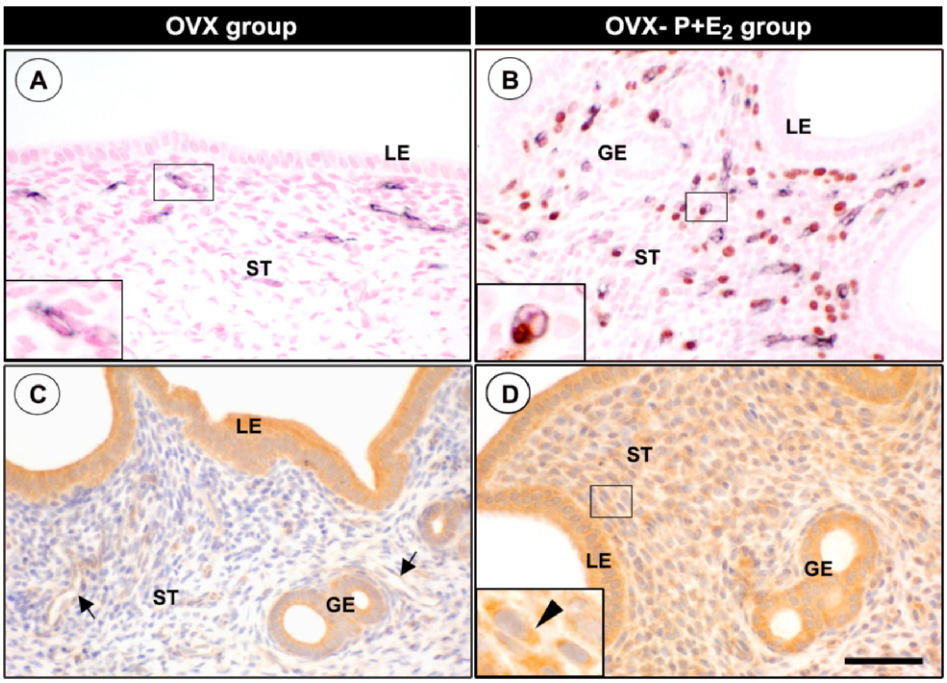

FIG. 2. Representative photomicrographs of uterine endothelial cell proliferation and VEGF expression induced by ovarian steroids in an OVX adult rat model in response to the P4 plus E_2 protocol. Endothelial cell proliferation was evaluated by BrdU incorporation in the uterus of OVX (**A**) and OVX-P+E_2 (**B**) rats. The inset in **A** shows a blood vessel with very low nestin expression and undetectable cellular proliferation; in **B**, the inset shows a blood vessel with nestin-positive endothelial cells (black cytoplasm) and a BrdU-positive cell (brown nucleus). **C**) VEGF immnunostaining was localized mainly in luminal and glandular epithelium and endothelium (arrows) of OVX rat uterus. **D**) An increased VEGF expression was detected on the subepithelial stroma of rats submitted to the P4 plus E_2 protocol. The inset in **D** shows at higher magnification cytoplasmic VEGF staining (arrowhead). GE, glandular epithelium; LE, luminal epithelium; ST, subepithelial stroma; P, progesterone. Bar = 50 μm. Original magnification ×1000 (insets in **A**, **B**, and **D**).

nized, rehydrated, and submitted to microwave antigen retrieval. To minimize the nonspecific background, sections were blocked for 1 h with normal goat serum (Sigma). The incubation with primary antibodies was performed overnight at 4°C. The secondary antibodies were incubated for 1 h, and then the sections were washed for a total of 45 min with three baths of PBS. Finally, all sections were washed in PBS and mounted with Vectashield fluorescent mounting medium (Vector Laboratories Inc., Burlingame, CA) with 4′,6-diamidino-2-phenylindole dihydrochoride (Fluka; Sigma) and stored in the dark at 4°C. Controls included uterine sections incubated using primary antibody buffer solution (3% bovine serum albumin, 0.1% Tween 20 in PBS) in place of the primary antibody to control for nonspecific staining. All immunostained sections were examined using an Olympus BX-51 microscope equipped for epifluorescence detection and with the appropriate filters (Olympus). Images were recorded using a high-resolution USB 2.0 Digital Color Camera (QImaging Go-3; QImaging, Surrey, BC, Canada).

Statistical Analysis

All data were calculated as the mean ± SEM. We performed a Kruskal-Wallis test to assess the overall significance (testing the hypothesis that the response was not homogeneous across treatments), and the Dunn posthoc test was used to compare each experimental group with the control group. Correlations were performed using Spearman analysis. $P < 0.05$ was considered statistically significant.

RESULTS

Endothelial Proliferation and VEGF Expression in the Uterus of Adult OVX Rats Submitted to Ovarian Steroid Treatment

First, we wanted to establish the normal response in the uterus of adult OVX rats treated with ovarian steroids on endothelial cell proliferation and VEGF expression. A pilot study was designed to compare adult OVX rats submitted to treatment with P4 and E_2 (denoted the OVX-P4 + E_2) to OVX rats treated with oil (denoted the OVX group). Endothelial cells were characterized by morphological features and by cytoplasmic nestin expression. The development of a double-IHC protocol allowed us to differentiate proliferating endothelial cells from proliferating stromal cells. As is shown in Figure 2A, BrdU labeling was undetectable in endothelial cells of OVX rats injected with vehicle (OVX group). After treatment with P4 and E_2 (OVX-P4 + E_2 group), the BrdU incorporation in endothelial cells increased markedly (Fig. 2B). The immunohistochemical analysis showed that OVX rats without hormonal stimulus exhibited VEGF expression in the luminal and glandular epithelium, with a slightly less intense staining in the endothelium (Fig. 2C). Notably, when the animals were treated with P4 plus E_2, a clear upregulation of VEGF expression was evident, mainly in the subepithelial stroma (Fig. 2, C vs. D).

Long-Term Effects of Neonatal Xenoestrogen Exposure on Uterine Endothelial Cell Proliferation and Vegf Expression

We evaluated whether neonatal exposure to BPA or DES alters endothelial proliferation, using the model of OVX adult rats submitted to P4 plus E_2 treatment. The results revealed an impaired endothelial proliferative response in rats exposed to both xenoestrogens. The percentage of endothelial cells that incorporated BrdU was significantly lower in BPA.05-, BPA20- and DES-exposed animals (16.90% ± 2.05%, 17.8% ± 1.16%, and 14.43% ± 1.9%, respectively) compared with control oil-exposed rats (22.83% ± 1.45%; $P < 0.05$). Figure 3 shows photomicrographs of BrdU/nestin immunostaining and the results of the quantification of endothelial proliferation. Even though in the subepithelial stroma the proliferative activity of endothelial cells diminished in xenoestrogen-exposed rats, the VWF-positive and nestin-expressing vascular areas were not different along experimental groups (Fig. 4).

Additionally, we evaluated the uterine *Vegf* expression in the same animals. We observed a significant decrease in *Vegf* mRNA levels in rats that were neonatally exposed to BPA.05, BPA20, and DES ($P < 0.05$; Fig. 5A). Then, we examined the expression of alternative splice variants of *Vegf* mRNA by RT-PCR using oligonucleotide primers that encompass exons 6 and 7 (Table 1). Three different splice variants of *Vegf* mRNA (*Vegf_120*, *Vegf_164*, and *Vegf_188*) were detected in the uteri of all experimental groups (Fig. 5B). The relative expression levels of these transcripts were *Vegf_164* > *Vegf_120* > *Vegf_188*, and the relative contribution of each other to the total expression of the *Vegf* gene did not show any change,

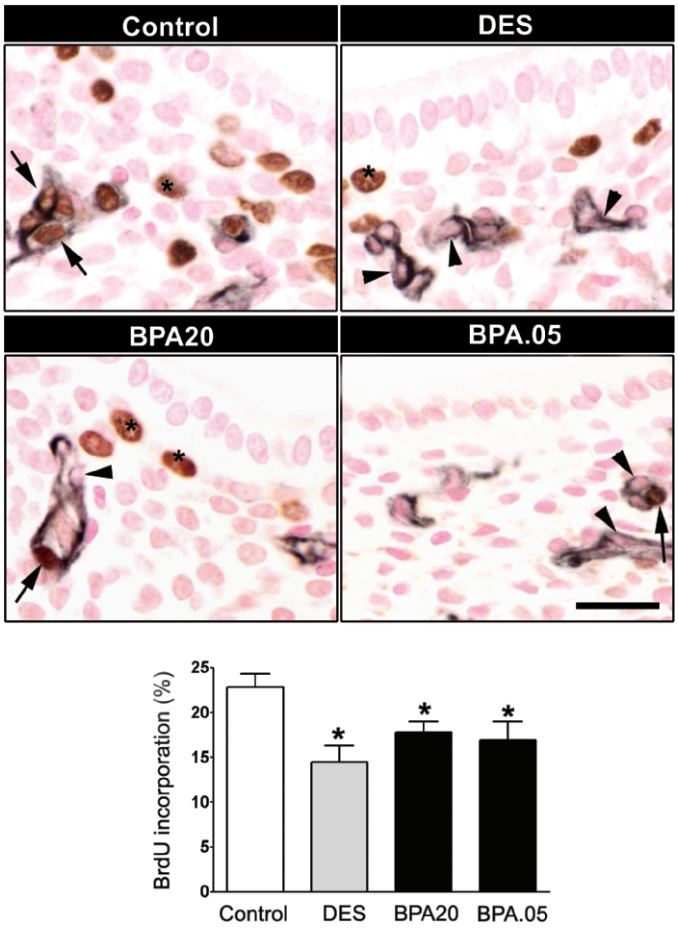

FIG. 3. Effect of neonatal exposure to xenoestrogens on endothelial cell proliferation in the uterus of OVX rats after P4 plus E_2 treatment. Representative photomicrographs of uterine sections double immunostained for BrdU (brown nuclei) and nestin (black cytoplasm) are shown. Note the decreased BrdU endothelial incorporation in rats neonatally exposed to DES, BPA20, and BPA.05 compared with control rats. Arrows indicate double-positive cells (proliferating endothelial cells), and arrowheads indicate endothelial cells (only positive for nestin in the cytoplasm, with pink nucleus counterstained with nuclear fast red). Asterisks in the photomicrographs indicate BrdU-positive fibroblastic stromal cells. Bar = 30 μm. The bar graph shows the quantification of endothelial proliferation evaluated on a total of 100 nestin-positive vessels located in the subepithelial stroma. Bars represent mean ± SEM. Control group, OVX-P4 + E_2. Asterisks in the graph signify $P < 0.05$.

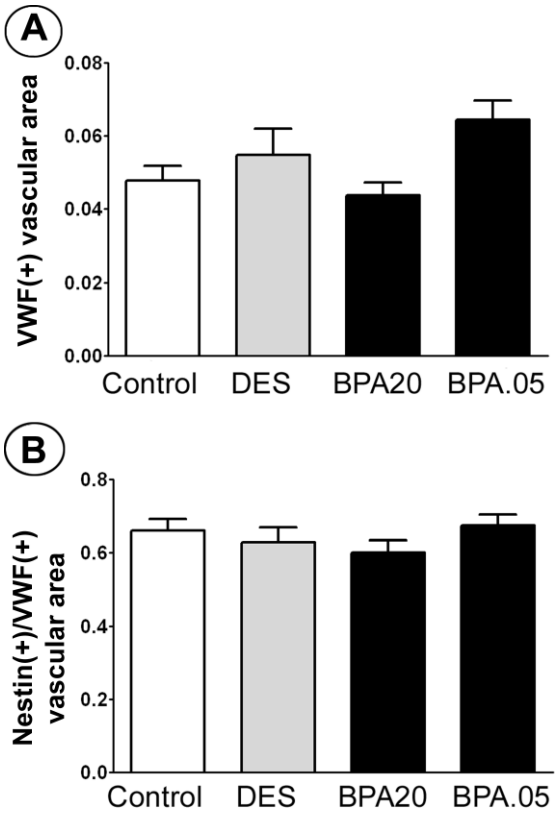

FIG. 4. Effect of neonatal exposure to xenoestrogens on vascular area in the uterus of OVX rats after P4 plus E_2 treatment. Quantification of VWF (**A**) and nestin-positive vascular areas (**B**) in the subepithelial stroma in each experimental group. Bars represent mean ± SEM.

suggesting that the splicing mechanism of the *Vegf* mRNA was not modified by neonatal exposure to xenoestrogens. Next, to evaluate VEGF protein expression, we performed an IHC assay. It showed that in rats neonatally exposed to xenoestrogens, the VEGF subepithelial expression was lower than in controls (Fig. 5, C and D). Moreover, *Vegf* mRNA expression was positively correlated with endothelial cell proliferation along the experimental groups ($P < 0.05$; Fig. 5E).

The Neonatal Xenoestrogen Exposure Alters the Endocrine Pathways in Response to Ovarian Steroid Treatment

ESR1 and PGR expressions in response to ovarian steroid treatment were evaluated in the subepithelial stroma and in the endothelial compartment as key mediators of steroid-hormone action. Representative photographs of ESR1- and PGR-immunostained uterine tissue sections are shown in Figure 6. In rats neonatally exposed to DES and BPA.05, the ESR1 subepithelial expression was lower than in controls (neonatally exposed to oil), whereas the BPA20 group showed no difference compared with the control (Fig. 6A). Regarding subepithelial PGR expression, females exposed to BPA did not differ from the controls in their response to the OVX-P4 + E_2 protocol (Fig. 6C). However, DES-exposed rats showed a lower PGR expression (Fig. 6C). The steroid receptor expression on endothelial cells was evaluated using double-IHC assays, which detected ESR1 or PGR in nestin-positive vascular areas. Notably, only BPA.05-exposed females showed fewer ESR1-positive endothelial cells relative to control rats (Fig. 6B). The percentage of PGR-positive endothelial cells did not show differences between the control and xenoestrogen-treated groups (Fig. 6D).

Two nuclear receptor coregulators were evaluated to obtain more information about the effects of neonatal xenoestrogen exposure on steroid pathways. NCOA3 (a coactivator) and NCOR1 (a corepressor) were detected by IHC in uterine samples obtained from control and xenoestrogen-exposed rats. In control conditions, NCOR1 immunostaining on subepithelial stroma showed a weak nuclear and cytoplasmic (perinuclear) expression, whereas NCOA3 was primarily found in the nuclei of subepithelial stromal cells. Specific staining was absent when primary antibodies were preincubated with peptides used as immunogens or replaced with normal rabbit serum. In rats neonatally exposed to BPA (BPA20 and BPA.05), a higher expression of NCOR1 corepressor was evidenced in the subepithelial stromal cells relative to control rats ($P < 0.05$; Fig. 7A). Regarding NCOA3 expression, rats neonatally exposed to xenoestrogens were similar to controls (Fig. 7B).

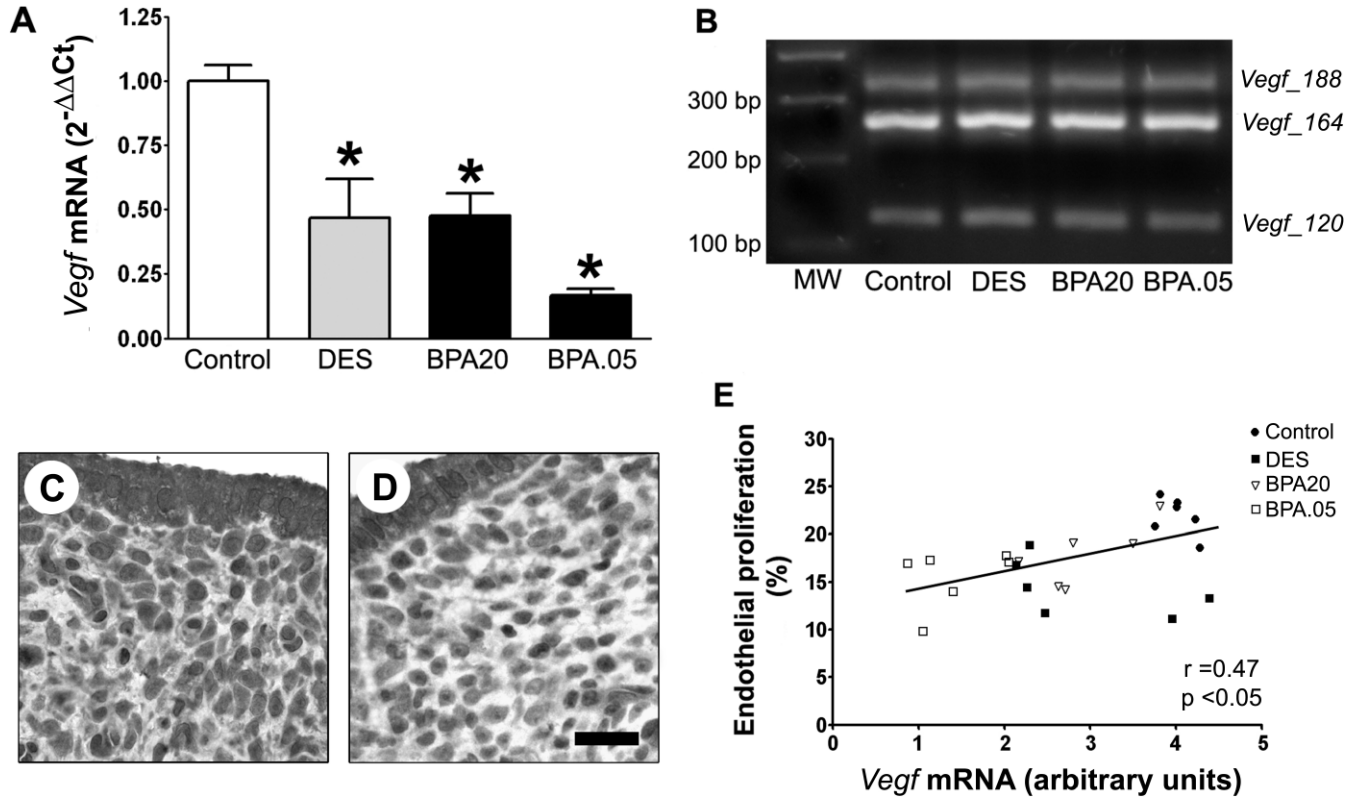

FIG. 5. Effect of neonatal exposure to xenoestrogens on *Vegf* mRNA, their splice variant expression, and protein expression in the uterus of OVX rats after P4 plus E_2 treatment. **A**) Relative *Vegf* mRNA levels were measured by real-time RT-PCR, and fold expression from control values was calculated by equation $2^{-\Delta\Delta CT}$. Control values were assigned to a reference level of 1. Bars represent mean values ± SEM. Asterisks denote $P < 0.05$. **B**) Representative 2% (w/v) agarose gel stained with ethidium bromide showing RT-PCR products from uteri corresponding to different experimental groups. Bands correspond to three major variants of *Vegf* mRNA in the rat: 120 (126 bp), 164 (258 bp), and 188 (330 bp). MW, molecular weight marker. Photomicrographs show VEGF protein expression in uterine samples of OVX-P4 + E_2 controls (**C**) and neonatally BPA.05-exposed rat (**D**). Bar = 30 μm. **E**) *Vegf* mRNA expression was positively correlated with endothelial cell proliferation in control and xenoestrogen-exposed groups ($P < 0.05$, Spearman correlation test).

Colocalization of VEGF and Mediator of Endocrine Pathway

Next, we wanted to know whether the observed changes in the endocrine pathway's mediators may be associated with changes in VEGF expression. To answer this question, we applied double-labeled immunofluorescent staining to investigate whether VEGF, ESR1, and NCOR1 proteins were expressed by the same cells in the uterine subepithelial compartment. The merged images show the coexpression of VEGF/ESR1, VEGF/NCOR1, or NCOR1/ESR1 in the uterine subepithelial stroma of a control and a BPA.05-exposed animal (Fig. 8). The dual-immunofluorescence assays for VEGF/ESR1 clearly revealed that in the control uteri, a high number of stromal cells coexpressed these proteins. In addition, a low expression of NCOR1 was detected in the same compartment. In contrast, the uteri of BPA.05-exposed rats showed an inverse pattern of expression, with low levels of VEGF and ESR1 expression and a high level of NCOR1 (Fig. 8). The results indicate that both low ESR1 expression and/or high NCOR1 expression detected in the BPA.05-exposed rats could be associated with the disruption of ovarian steroid-VEGF induction.

DISCUSSION

The endothelial cell is of utmost importance for the proper functioning of the female reproductive tract. Disturbances of reproductive functions due to environmental contaminant exposure urge the investigation of possible effects of endocrine disrupters on this cell population. In the present study, we demonstrated that the proliferative response of the uterine endothelial cells to ovarian steroids during adulthood is altered by neonatal exposure to low doses of BPA and DES. Moreover, xenoestrogen exposure downregulated VEGF expression in the subepithelial uterine stroma, another event closely related to control of the vascular compartment.

There is considerable evidence from in vivo studies demonstrating that early BPA exposure can exert important changes on the rodent reproductive female tract and mammary gland long after the period of exposure has ended [16, 29, 34]. Most of these alterations may be related to disruption of ovarian steroid-regulated gene expression. Recently, we demonstrated that neonatal BPA exposure impaired the uterine stroma proliferation in response to ovarian steroids in adult rats, an effect that was associated with *Hoxa10* suppression [16]. These alterations could affect uterine receptivity and decidualization.

Given that uterine vascularization is another key process in the preparation of the endometrium to embryo implantation, here we investigated whether neonatal xenoestrogen exposure affects the vascular compartment. In response to ovarian steroid treatment, female rats neonatally exposed to xenoestrogens showed a decreased induction of uterine endothelial proliferation without changes in nestin expression or in the total vascular area measured by VWF. This apparent

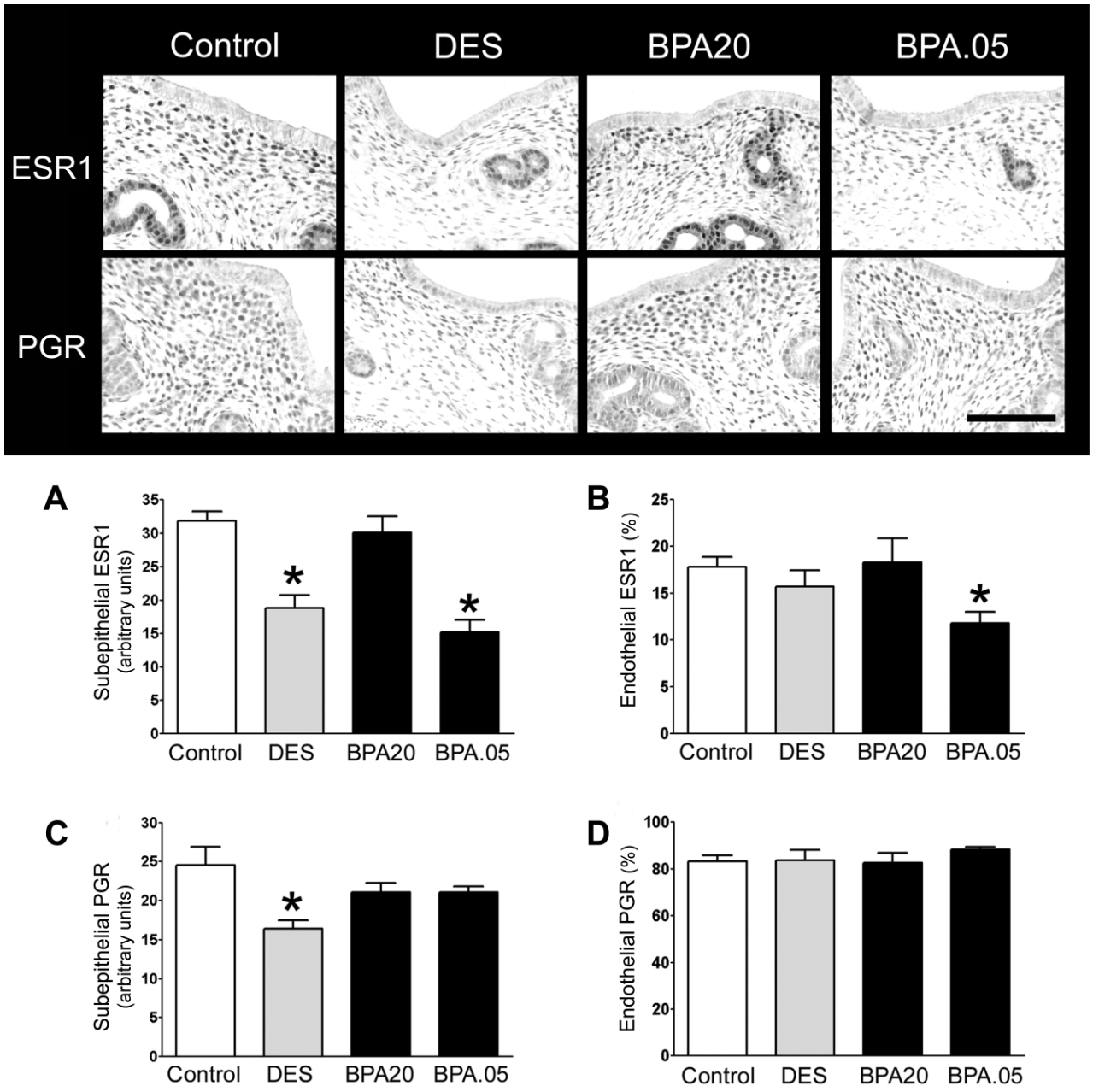

FIG. 6. Effect of neonatal exposure to DES or BPA on steroid receptor expression in the uterus of OVX rats after P4 plus E_2 treatment. Photomicrographs show uterine sections immunostained for ESR1 and PGR. These images were obtained from sections without hematoxylin counterstaining. Bar = 150 μm. Quantification of subepithelial ESR1 (ERα; **A**), subepithelial PGR (PR; **B**), endothelial ESR1 (**C**), and endothelial PGR (**D**) expression in each experimental group. Quantification of subepithelial steroid receptor expression was performed by image analysis evaluating the IOD on tissue sections without counterstaining. The results were expressed as relative units. On the other hand, the quantification of the percentage of endothelial steroid receptor expression was performed on double-immunostained sections (PGR/nestin or ESR1/nestin). Bars represent mean ± SEM. Asterisks denote $P < 0.05$.

discordance could be owing to the fact that rats were killed just 20 h after the last hormone injection. We suggest that this short period of time could not be enough to observe changes in vascular area, even though the proliferation rate was different between control and xenoestrogen-treated animals.

We also investigated whether neonatal exposure to xenoestrogens affects VEGF expression, which is a recognized regulator of vascular compartment. Our results demonstrated that xenoestrogen exposure decreased *Vegf* mRNA expression in response to P4 plus E_2 treatment. It is well known that VEGF is a secreted growth factor that operates by binding to specific receptors and that the VEGF/receptor signaling system is mainly involved in the regulation of endothelial cell proliferation [35]. Therefore, our results suggest that the alteration in steroid-mediated activation of *Vegf* could be responsible for the impaired endothelial proliferative response found in xenoestrogen-exposed rats. Because there were no changes in the processing of the *Vegf* mRNA splice variants, this suggests that xenoestrogens could modify *Vegf* mRNA expression by acting at the primary transcript level.

Until now, little has been known about the endocrine disrupter's effects on uterine endothelial proliferation and VEGF expression. Bredhult et al. [36] studied whether endocrine-disrupting chemicals affect the proliferation and viability of human endometrial endothelial cells in vitro. In accordance with our results, the authors observed that after

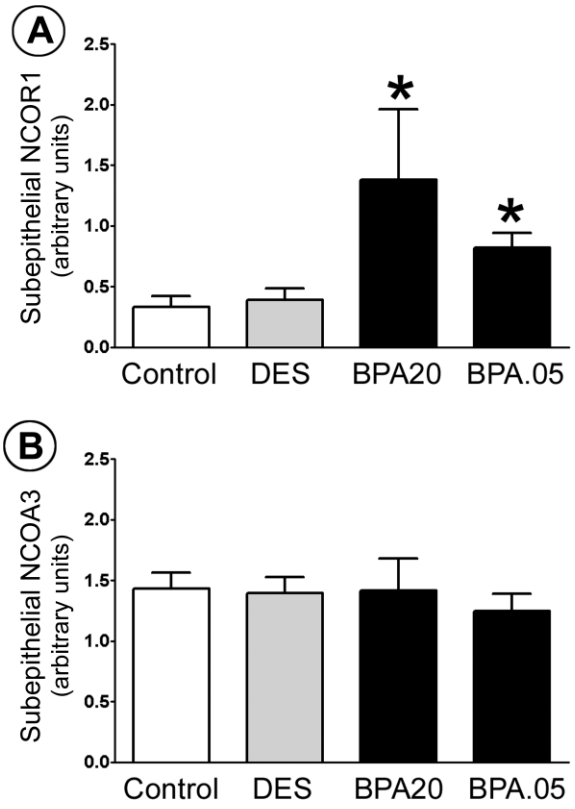

FIG. 7. Effect of neonatal exposure to xenoestrogens on coregulator expression in the uterus of OVX rats after P4 plus E_2 treatment. Immunohistochemical quantification of NCOR1 (**A**) and NCOA3 (**B**) in the uterine subepithelial compartment of OVX-P4 + E_2 rats. Bars represent mean ± SEM. Asterisks denote $P < 0.05$.

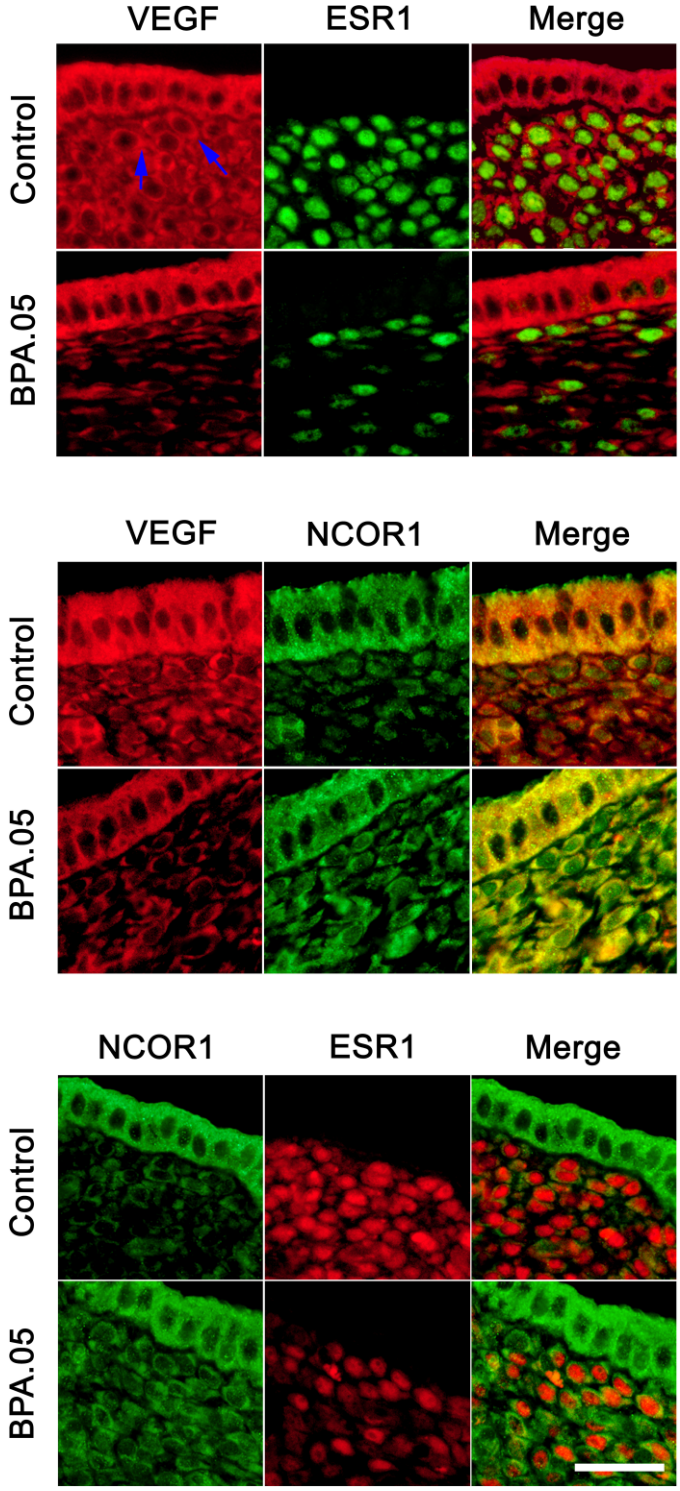

FIG. 8. Colocalization of VEGF, ESR1 (ERα), and NCOR1 in the uterus of OVX rats after P4 plus E_2 treatment. Top panels show dual-immunofluorescence staining for VEGF/ESR1 VEGF labeling is indicated by red, ESR1 labeling is indicated by green, and the digitally combined image (merge) shows that the lower expression of VEGF in BPA.05 animals is coincident with a lower expression of ESR1. Arrows show cytoplasmic VEGF staining. Middle panels show dual-immunofluorescence staining for VEGF/NCOR1. VEGF labeling is indicated by red, NCOR1 labeling is indicated by green, and combined labeling is indicated by yellow-orange (merge). The digitally combined image (merge) shows that the lower expression of VEGF in BPA.05 animals is associated with a higher expression of NCOR1 in the same compartment. Bottom panels show dual immunofluorescence staining for NCOR1/ESR1. NCOR1 labeling is indicated by green, and ESR1 labeling is indicated by red. The merge image shows that NCOR1 colocalizes with ESR1 in the same cells. Bar = 30 μm.

treatment with 0.01, 1, or 100 μM BPA, endothelial proliferation was lower than in the control. However, in contrast to our observations, the adult OVX rats treated with BPA by i.p. injection of 0.02–150 mg/kg body weight had a rapid induction of *Vegf* expression in the uterus, the vagina, and the pituitary [17]. Also, in vitro results showed that genistein and BPA upregulated *Vegf* expression in MELN cells by an ESR-dependent mechanism [18]. Discrepancies between these results and ours may be attributable in part to limitations of the in vitro assays that are of narrow predictive value compared with in vivo analysis [37]. Also, it is well known that the route of administration of BPA has an impact on the pharmacokinetics only in the adults and not in fetal or neonatal rodents, because the developing neonatal liver does not have the capacity to metabolize BPA as does the adult liver [38–40]. Therefore, findings obtained from different reports may be influenced by the life stage in which exposure occurred and also by the administration route employed. Finally, it is worth noting that our results were observed in animals neonatally exposed to two different doses of BPA, of which one mimics the reference dose currently considered "safe" for daily human intake (50 μg/kg per day) according to the U.S. Environmental Protection Agency [41]. Moreover, it is less than the cutoff dose (5 mg/kg per day) recently established by the National Toxicology Program for low-dose studies [12].

Hormonal regulation of VEGF has been reported in multiple tissues, and whether there are increases or decreases in expression depends on the cell context. Any particular cellular response could be due, in part, to differential expression of steroid receptors and/or other nuclear transcription factors and/

or their interactions with regulatory elements [42]. Kazi et al. [43] demonstrated that E_2, through its receptor (ESR1), rapidly stimulates *Vegf* expression in the rat uterus at the transcriptional level. They showed by chromatin immunoprecipitation that E_2 induced an increase in transcription factor Sp1 binding and the recruitment of ESR1 to a proximal, GC-rich region of the *Vegf* promoter [43]. Based on these findings, we investigated whether the neonatal BPA or DES exposure could alter the normal expression of ESR1 and PGR in the adult uteri. The DES- and BPA.05-exposed animals showed a decreased ESR1 expression in the uterine subepithelial stroma, whereas the percentage of ESR1 in the endothelial compartment decreased only in BPA.05-treated rats. In contrast, PGR expression showed no changes in the subepithelial stroma or in endothelial cells after P4 plus E_2 stimulation. Therefore, we suggest that disturbed *Vegf* expression could be the result of changes in endocrine pathways, such as an altered induction of ESR1 expression.

Coregulator proteins serve as partners for nuclear receptors, orchestrating the molecular events required for receptor-dependent transcriptional regulation [44]. Therefore, the sensitivity to steroid hormones also depends on the availability of steroid receptor coregulators [45]. Our data demonstrated that neonatal exposure to BPA affected uterine stromal NCOR1 expression in response to P4 plus E_2 treatment, showing a clear upregulation of this corepressor in the subepithelial compartment. Moreover, immunofluorescence results showed that NCOR1 and ESR1 are present in the same uterine cells. Nuclear receptor coregulators were revealed as targets for endocrine disrupters, as shown for NCOR in the prostate and NCOA1 in the uterus [45, 46]. The increase of NCOR1 observed here may have implications for gene expression on a broad scale because NCOR1 is recruited by many transcription factors, including steroid receptors [44], and it is also a limiting factor inhibiting transcriptional activity of steroid hormone receptors [47]. Because the abnormal overexpression of NCOR1 was found in the same subepithelial stromal cells where VEGF induction failed, this suggests that the high levels of NCOR1 could interfere with different steroid-dependent genes in xenoestrogen-exposed animals. This conclusion is supported by the recently published results from our group [16] that show an impaired uterine proliferative response to steroid treatment associated with a silencing of *Hoxa10*, together with the increased stromal expression of NCOR1.

Finally, greater effects of the low dose of BPA are consistent with a nonmonotonic, inverted-U-shaped dose-response curve. Several reports support the notion that endocrine disrupters, such as BPA, produce biological effects exhibiting nonmonotonic dose-response curves [48–52].

VEGF plays a pivotal role in the regulation of uterine microvascular permeability and angiogenesis in the implantation process [35, 53]. Therefore, our results using a model that mimicked the hormonal milieu of the preimplantation period suggest that neonatal BPA exposure might have negative consequences on female fertility, thereby impairing embryo implantation.

ACKNOWLEDGMENTS

We are grateful to Juan Grant and Juan C. Villarreal for technical assistance and animal care, and Dr. Adriana Pereyra for technical help in antibody production.

REFERENCES

1. Perrot-Applanat M, Deng M, Fernandez H, Lelaidier C, Meduri G, Bouchard P. Immunohistochemical localization of estradiol and progesterone receptors in human uterus throughout pregnancy: expression in endometrial blood vessels. J Clin Endocrinol Metab 1994; 78:216–224.
2. Lecce G, Meduri G, Ancelin M, Bergeron C, Perrot-Applanat M. Presence of estrogen receptor beta in the human endometrium through the cycle: expression in glandular, stromal, and vascular cells. J Clin Endocrinol Metab 2001; 86:1379–1386.
3. Weitlauf HM. Biology of implantation. In: Knobil E, Neill JD (eds.), The Physiology of Reproduction. New York: Raven Press; 1994:391–440.
4. Rabbani ML, Rogers PA. Role of vascular endothelial growth factor in endometrial vascular events before implantation in rats. Reproduction 2001; 122:85–90.
5. Rockwell LC, Pillai S, Olson CE, Koos RD. Inhibition of vascular endothelial growth factor/vascular permeability factor action blocks estrogen-induced uterine edema and implantation in rodents. Biol Reprod 2002; 67:1804–1810.
6. Sengupta J, Lalitkumar PG, Najwa AR, Charnock-Jones DS, Evans AL, Sharkey AM, Smith SK, Ghosh D. Immunoneutralization of vascular endothelial growth factor inhibits pregnancy establishment in the rhesus monkey (*Macaca mulatta*). Reproduction 2007; 133:1199–1211.
7. Shweiki D, Itin A, Neufeld G, Gitay-Goren H, Keshet E. Patterns of expression of vascular endothelial growth factor (VEGF) and VEGF receptors in mice suggest a role in hormonally regulated angiogenesis. J Clin Invest 1993; 91:2235–2243.
8. Karuri AR, Kumar AM, Mukhopadhyay D. Differential expression and selective localization of vascular permeability factor/vascular endothelial growth factor in the rat uterus during the estrous cycle. J Endocrinol 1998; 159:489–499.
9. Yi XJ, Jiang HY, Lee KK, O WS, Tang PL, Chow PH. Expression of vascular endothelial growth factor (VEGF) and its receptors during embryonic implantation in the golden hamster (*Mesocricetus auratus*). Cell Tissue Res 1999; 296:339–349.
10. Kazi AA, Koos RD. Estrogen-induced activation of hypoxia-inducible factor-1alpha, vascular endothelial growth factor expression, and edema in the uterus are mediated by the phosphatidylinositol 3-kinase/Akt pathway. Endocrinology 2007; 148:2363–2374.
11. Mueller MD, Vigne JL, Pritts EA, Chao V, Dreher E, Taylor RN. Progestins activate vascular endothelial growth factor gene transcription in endometrial adenocarcinoma cells. Fertil Steril 2003; 79:386–392.
12. Chapin RE, Adams J, Boekelheide K, Gray LE Jr, Hayward SW, Lees PS, McIntyre BS, Portier KM, Schnorr TM, Selevan SG, Vandenbergh JG, Woskie SR. National Toxicology Program/Center for the Evaluation of Risks to Human Reproduction expert panel report on the reproductive and developmental toxicity of bisphenol A. Birth Defects Res B Dev Reprod Toxicol 2008; 83:157–395.
13. Yamamoto T, Yasuhara A. Quantities of bisphenol A leached from plastic waste samples. Chemosphere 1999; 38:2569–2576.
14. Schonfelder G, Friedrich K, Paul M, Chahoud I. Developmental effects of prenatal exposure to bisphenol a on the uterus of rat offspring. Neoplasia 2004; 6:584–594.
15. Markey CM, Coombs MA, Sonnenschein C, Soto AM. Mammalian development in a changing environment: exposure to endocrine disruptors reveals the developmental plasticity of steroid-hormone target organs. Evol Dev 2003; 5:67–75.
16. Varayoud J, Ramos JG, Bosquiazzo VL, Muñoz-de-Toro M, Luque EH. Developmental exposure to Bisphenol a impairs the uterine response to ovarian steroids in the adult. Endocrinology 2008; 149:5848–5860.
17. Long X, Burke KA, Bigsby RM, Nephew KP. Effects of the xenoestrogen bisphenol A on expression of vascular endothelial growth factor (VEGF) in the rat. Exp Biol Med (Maywood) 2001; 226:477–483.
18. Buteau-Lozano H, Velasco G, Cristofari M, Balaguer P, Perrot-Applanat M. Xenoestrogens modulate vascular endothelial growth factor secretion in breast cancer cells through an estrogen receptor-dependent mechanism. J Endocrinol 2008; 196:399–412.
19. Rider V, Thomson E, Seifert C. Transit of rat uterine stromal cells through G1 phase of the cell cycle requires temporal and cell-specific hormone-dependent changes on cell cycle regulators. Endocrinology 2003; 144: 5450–5458.
20. Ramos JG, Varayoud J, Monje L, Moreno-Piovano G, Muñoz-de-Toro M, Luque EH. Diethylstilbestrol alters the population dynamic of neural precursor cells in the neonatal male rat dentate gyrus. Brain Res Bull 2007; 71:619–627.
21. Kashida S, Sugino N, Takiguchi S, Karube A, Takayama H, Yamagata Y, Nakamura Y, Kato H. Regulation and role of vascular endothelial growth factor in the corpus luteum during mid-pregnancy in rats. Biol Reprod 2001; 64:317–323.
22. Chan YL, Lin A, McNally J, Peleg D, Meyuhas O, Wool IG. The primary structure of rat ribosomal protein L19. A determination from the sequence

of nucleotides in a cDNA and from the sequence of amino acids in the protein. J Biol Chem 1987; 262:1111–1115.
23. Higuchi R, Fockler C, Dollinger G, Watson R. Kinetic PCR analysis: real-time monitoring of DNA amplification reactions. Biotechnology 1993; 11: 1026–1030.
24. Bosquiazzo VL, Ramos JG, Varayoud J, Muñoz-de-Toro M, Luque EH. Mast cell degranulation in rat uterine cervix during pregnancy correlates with expression of vascular endothelial growth factor mRNA and angiogenesis. Reproduction 2007; 133:1045–1055.
25. Eckhart L, Ban J, Ballaun C, Weninger W, Tschachler E. Reverse transcription-polymerase chain reaction products of alternatively spliced mRNAs form DNA heteroduplexes and heteroduplex complexes. J Biol Chem 1999; 274:2613–2615.
26. Muñoz-de-Toro M, Maffini MV, Giardina RH, Luque EH. Processing fine needle aspirates of prostate carcinomas for standard immunocytochemical studies and in situ apoptosis detection. Pathol Res Pract 1998; 194:631–636.
27. Ramos JG, Varayoud J, Kass L, Rodriguez H, Costabel L, Muñoz-de-Toro M, Luque EH. Bisphenol a induces both transient and permanent histofunctional alterations of the hypothalamic-pituitary-gonadal axis in prenatally exposed male rats. Endocrinology 2003; 144:3206–3215.
28. Varayoud J, Ramos JG, Bosquiazzo VL, Muñoz-de-Toro M, Luque EH. Mast cells degranulation affects angiogenesis in the rat uterine cervix during pregnancy. Reproduction 2004; 127:379–387.
29. Durando M, Kass L, Piva J, Sonnenschein C, Soto AM, Luque EH, Muñoz-de-Toro M. Prenatal bisphenol A exposure induces preneoplastic lesions in the mammary gland in Wistar rats. Environ Health Perspect 2007; 115:80–86.
30. Mokrý J, Cízková D, Filip S, Ehrmann J, Osterreicher J, Kolár Z, English D. Nestin expression by newly formed human blood vessels. Stem Cells Dev 2004; 13:658–664.
31. Takahashi N, Itoh MT, Ishizuka B. Human chorionic gonadotropin induces nestin expression in endothelial cells of the ovary via vascular endothelial growth factor signaling. Endocrinology 2008; 149:253–260.
32. Ramos JG, Varayoud J, Bosquiazzo VL, Luque EH, Muñoz-de-Toro M. Cellular turnover in the rat uterine cervix and its relationship to estrogen and progesterone receptor dynamics. Biol Reprod 2002; 67:735–742.
33. Kass L, Varayoud J, Ortega H, Muñ oz de Toro M, Luque EH. Detection of bromodeoxyuridine in formalin-fixed tissue. DNA denaturation following microwave or enzymatic digestion pretreatment is required. Eur J Histochem 2000; 44:185–191.
34. Muñoz-de-Toro M, Markey CM, Wadia PR, Luque EH, Rubin BS, Sonnenschein C, Soto AM. Perinatal exposure to bisphenol-A alters peripubertal mammary gland development in mice. Endocrinology 2005; 146:4138–4147.
35. Ferrara N, Gerber HP, LeCouter J. The biology of VEGF and its receptors. Nat Med 2003; 9:669–676.
36. Bredhult C, Bäcklin BM, Olovsson M. Effects of some endocrine disruptors on the proliferation and viability of human endometrial endothelial cells in vitro. Reprod Toxicol 2007; 23:550–559.
37. Schlumpf M, Cotton B, Conscience M, Haller V, Steinmann B, Lichtensteiger W. In vitro and in vivo estrogenicity of UV screens. Environ Health Perspect 2001; 109:239–244.
38. Upmeier A, Degen GH, Diel P, Michna H, Bolt HM. Toxicokinetics of bisphenol A in female DA/Han rats after a single i.v. and oral administration. Arch Toxicol 2000; 74:431–436.
39. Tominaga T, Negishi T, Hirooka H, Miyachi A, Inoue A, Hayasaka I, Yoshikawa Y. Toxicokinetics of bisphenol A in rats, monkeys and chimpanzees by the LC-MS/MS method. Toxicology 2006; 226:208–217.
40. Taylor JA, Welshons WV, Vom Saal FS. No effect of route of exposure (oral; subcutaneous injection) on plasma bisphenol A throughout 24h after administration in neonatal female mice. Reprod Toxicol 2008; 25:169–176.
41. Environmental Protection Agency. Bisphenol A (CASRN 80-05-7). In:Integrated Risk Information System Substance, U.S. Environmental Protection Agency, Washington, DC. 2008. World Wide Web (URL: http://www.epa.gov/iris/subst/0356.htm). (April, 2008).
42. Stoner M, Wormke M, Saville B, Samudio I, Qin C, Abdelrahim M, Safe S. Estrogen regulation of vascular endothelial growth factor gene expression in ZR-75 breast cancer cells through interaction of estrogen receptor alpha and SP proteins. Oncogene 2004; 23:1052–1063.
43. Kazi AA, Jones JM, Koos RD. Chromatin immunoprecipitation analysis of gene expression in the rat uterus in vivo: estrogen-induced recruitment of both estrogen receptor alpha and hypoxia-inducible factor 1 to the vascular endothelial growth factor promoter. Mol Endocrinol 2005; 19: 2006–2019.
44. Hall JM, McDonnell DP. Coregulators in nuclear estrogen receptor action: from concept to therapeutic targeting. Mol Interv 2005; 5:343–357.
45. Durrer S, Ehnes C, Fuetsch M, Maerkel K, Schlumpf M, Lichtensteiger W. Estrogen sensitivity of target genes and expression of nuclear receptor co-regulators in rat prostate after pre- and postnatal exposure to the ultraviolet filter 4-methylbenzylidene camphor. Environ Health Perspect 2007; 115(suppl 1):42–50.
46. Durrer S, Maerkel K, Schlumpf M, Lichtensteiger W. Estrogen target gene regulation and coactivator expression in rat uterus after developmental exposure to the ultraviolet filter 4-methylbenzylidene camphor. Endocrinology 2005; 146:2130–2139.
47. Privalsky ML. The role of corepressors in transcriptional regulation by nuclear hormone receptors. Annu Rev Physiol 2004; 66:315–360.
48. Nishizawa H, Morita M, Sugimoto M, Imanishi S, Manabe N. Effects of in utero exposure to bisphenol A on mRNA expression of arylhydrocarbon and retinoid receptors in murine embryos. J Reprod Dev 2005; 51:315–324.
49. vom Saal FS, Hughes C. An extensive new literature concerning low dose effects of bisphenol A shows the need for a new risk assessment. Environ Health Perspect 2005; 113:926–933.
50. Wetherill YB, Fisher NL, Staubach A, Danielsen M, Vere White RW, Knudsen KE. Xenoestrogen action in prostate cancer: pleiotropic effects dependent on androgen receptor status. Cancer Res 2005; 65:54–65.
51. Zsarnovszky A, Le HH, Wang HS, Belcher SM. Ontogeny of rapid estrogen mediated extracellular signal regulated kinase signaling in the rat cerebellar cortex: potent nongenomic agonist and endocrine disrupting activity of the xenoestrogen bisphenol A. Endocrinology 2005; 146:5388–5396.
52. Monje L, Varayoud J, Luque EH, Ramos JG. Neonatal exposure to bisphenol A modifies the abundance of estrogen receptor alpha transcripts with alternative 5'-untranslated regions in the female rat preoptic area. J Endocrinol 2007; 194:201–212.
53. Halder JB, Zhao X, Soker S, Paria BC, Klagsbrun M, Das SK, Dey SK. Differential expression of VEGF isoforms and VEGF(164)-specific receptor neuropilin-1 in the mouse uterus suggests a role for VEGF(164) in vascular permeability and angiogenesis during implantation. Genesis 2000; 26:213–224.